Inorg. Chem. **2008**, *47*, 5625−5633

Photosensitizer in a Molecular Bowl and its Effect on the DNA-Binding and -Cleavage Activity of 3d-Metal Scorpionates

Sovan Roy, Ashis K. Patra, Shanta Dhar, and Akhil R. Chakravarty*

Department of Inorganic & Physical Chemistry, Indian Institute of Science, Bangalore 560012, India

Received September 17, 2007

Ternary 3d-metal complexes $[M(Tp^{Ph})(B)](ClO_4)$ (**1**−**8**), where M is Co(II), Ni(II), Cu(II) and Zn(II), Tp^{Ph} is anionic tris(3-phenylpyrazolyl)borate, and B is *N,N*-donor heterocyclic base, namely, 1,10-phenanthroline (phen, **1**−**4**) and dipyrido[3,2-*d*:2′,3′-*f*]quinoxaline (dpq, **5**−**8**), were prepared from a reaction of the perchlorate salt of the metal with KTp^{Ph} and B in CH_2Cl_2. The complexes were characterized by various physicochemical methods. **4**−**6** and **8** were structurally characterized by single-crystal X-ray crystallography. The crystal structures of the complexes show the presence of discrete cationic complexes having a square-pyramidal (4 + 1) coordination geometry in which two nitrogen atoms of the phenanthroline base (B) and two nitrogen atoms of the Tp^{Ph} ligand occupy the basal plane and one nitrogen of the Tp^{Ph} ligand binds at the axial site. The phenyl groups of the Tp^{Ph} form a bowl-shaped structure that essentially encloses the {M(phen/dpq)} moiety. DNA-binding studies were carried out using various spectral techniques and from viscosity measurements. The complexes show moderate binding propensity to calf thymus DNA at the minor groove, giving binding constant values (K_b) of $\sim 10^4$ M^{-1}. The complexes exhibit poor DNA-cleavage activity in the dark in the presence of 3-mercaptopropionic acid (MPA) or hydrogen peroxide (H_2O_2). The photoinduced DNA-cleavage activity of the complexes was investigated using UV-A radiation of 365 nm and visible light of two different wavelengths with a tunable multicolor Ar−Kr mixed gas ion laser source. The dpq complexes show efficient photoinduced DNA-cleavage activity via a metal-assisted photoexcitation process involving the formation of singlet oxygen as the cleavage active species in a type-II pathway. The paramagnetic d^7−Co(II)−dpq and d^9−Cu(II)−dpq complexes exhibit efficient DNA-cleavage activity in visible light. The paramagnetic d^8−Ni(II)−dpq complex displays only minor DNA-cleavage activity in visible light. Diamagnetic d^{10}−Zn(II)−dpq complex shows only UV-A light-induced DNA cleavage but no apparent DNA-cleavage activity in visible light. Steric protection of the photoactive quinoxaline moiety of the dpq ligand inside the hydrophobic $\{M(Tp^{Ph})\}$ molecular bowl has a positive effect on the photoinduced DNA-cleavage activity.

Introduction

Tris(pyrazolyl)borate (Tp) is a versatile ligand in inorganic chemistry.[1–3] The tridentate capping ligand and its derivatives have been extensively used in biomimetic modeling of the active site structures of several metalloproteins, in the synthesis of organometallic complexes, and for designing novel catalysts in organic transformation reactions.[4–10] The versatility of this ligand arises from the variety of steric constraints that could be obtained by altering the substituents

* To whom correspondence should be addressed. E-mail: arc@ipc.iisc.ernet.in; Fax: 91-80-23600683.

(1) (a) Trofimenko, S. *J. Am. Chem. Soc.* **1966**, *88*, 1842. (b) Trofimenko, S. *Polyhedron* **2004**, *23*, 197. (c) Trofimenko, S. *Scorpionates: The Coordination Chemistry of Polypyrazolylborate Ligands*; Imperial College Press: London, 1999.

(2) (a) Kitajima, N.; Tolman, W. B. *Prog. Inorg. Chem.* **1995**, *43*, 419. (b) Hikichi, S.; Akita, M.; Moro-oka, Y. *Coord. Chem. Rev.* **2000**, *198*, 61.

(3) (a) Vahrenkamp, H. *Acc. Chem. Res.* **1999**, *32*, 589. (b) Parkin, G. *Chem. Rev.* **2004**, *104*, 699.

(4) (a) Blackman, A. G.; Tolman, W. B. In *Structure and Bonding*; Springer-Verlag: Heidelberg, Germany, 2000; *97* p 179. (b) Lippard, S. J. *Angew. Chem., Int. Ed. Engl.* **1988**, *27*, 344. (c) Armstrong, W. H.; Lippard, S. J. *J. Am. Chem. Soc.* **1983**, *105*, 4837. (d) Armstrong, W. H.; Spool, A.; Papaefthymiou, G. C.; Frankel, R. B.; Lippard, S. J. *J. Am. Chem. Soc.* **1984**, *106*, 3653. (e) Armstrong, W. H.; Lippard, S. J. *J. Am. Chem. Soc.* **1984**, *106*, 4632.

(5) (a) Kitajima, N.; Fujisawa, K.; Moro-oka, Y. *J. Am. Chem. Soc.* **1989**, *111*, 8975. (b) Hikichi, S.; Komatsuzaki, H.; Kitajima, N.; Akita, M.; Mukai, M.; Kitagawa, T.; Moro-oka, Y. *Inorg. Chem.* **1997**, *36*, 266. (c) Fujisawa, K.; Tanaka, M.; Moro-oka, Y.; Kitajima, N. *J. Am. Chem. Soc.* **1994**, *116*, 12079. (d) Kitajima, N.; Katayama, T.; Fujisawa, K.; Iwata, Y.; Moro-oka, Y. *J. Am. Chem. Soc.* **1993**, *115*, 7872.

10.1021/ic702508r CCC: $40.75
Published on Web 06/05/2008

at the 3- and 5- positions of the pyrazolyl ring in Tp. We have earlier used the phenyl substituted tris(pyrazolyl)borate anion (Tp^{Ph}) in designing ternary Cu(II) complexes $[Cu(Tp^{Ph})B]^+$ of phenanthroline bases (B) to explore the effect of steric encumbrance of the Tp^{Ph} ligand on the DNA-binding and -cleavage activity of the complexes.[11] It has been observed that the DNA-binding phenanthroline bases are sterically enclosed in the $\{Cu(Tp^{Ph})\}$ bowl, and, as a consequence, the complexes show only moderate DNA-binding propensity. The steric enclosure of the phenanthroline base also reduces the chemical nuclease activity of the Tp^{Ph} complexes in comparison to the bis(1,10-phenanthroline)copper(II) and bis(dipyridoquinoxaline)copper(II) analogues.[12,13]

In a subsequent communication, we have shown that such a steric encumbrance has, however, positive effects on the photoinduced DNA-cleavage activity of the complexes.[14] The dipyrido[3,2-*d*:2′,3′-*f*]quinoxaline (dpq) and dipyrido[3,2-*a*:2′,3′-*c*]phenazine (dppz) copper(II) complexes having respective photoactive quinoxaline and phenazine moiety cleave DNA on photoirradiation in red light by the singlet oxygen pathway. It is proposed that the hydrophobic molecular bowl of the $\{Cu(Tp^{Ph})\}$ moiety effectively encloses the photosensitizer thus making it inaccessible to the solvent molecules. This possibly leads to an enhancement of the DNA-photocleavage activity. The results are of importance because the use of scorpionate and related ligands in DNA-binding and -cleavage studies remains essentially unexplored.[15]

The present work stems from our interest to study the photoinduced DNA-cleavage activity of 3d-metal scorpionates using bivalent metal ions like Co(II), Ni(II), and Zn(II) besides the Cu(II) ion. The choice of the metal ions is based on their different electronic configurations, leading to significant differences in their physicochemical properties. The aim is to elucidate the effect of the electronic structure of the 3d-metal ions in the presence of sterically demanding Tp^{Ph} ligand on their DNA-cleavage activity in visible light. Transition-metal complexes showing visible light-induced DNA-cleavage activity are of importance in the chemistry of photodynamic therapy (PDT) of cancer.[16–20] Redox-active metal complexes showing cleavage of DNA in the presence of a reducing agent are generally cytotoxic due to the presence reducing thiols in the cellular medium.[20–24] Designing of metal-based compounds that show poor chemical nuclease activity but efficient photoinduced DNA-cleavage activity is a necessity for PDT to reduce the dark toxicity of

(6) (a) Pesavento, R. P.; Berlinguette, C. P.; Holm, R. H. *Inorg. Chem.* **2007**, *46*, 510. (b) Laughlin, L. J.; Eagle, A. A.; George, G. N.; Tiekink, E. R. T.; Young, C. G. *Inorg. Chem.* **2007**, *46*, 939. (c) Jacobsen, F. E.; Breece, R. M.; Myers, W. K.; Tierney, D. L.; Cohen, S. M. *Inorg. Chem.* **2006**, *45*, 7306. (d) Ibrahim, M. M.; Olmo, C. P.; Tekeste, T.; Seebacher, J.; He, G.; Calvo, J. A. M.; Boehmerle, K.; Steinfeld, G.; Brombacher, H.; Vahrenkamp, H, *Inorg. Chem.* **2006**, *45*, 7493.

(7) Marques, N.; Sella, A.; Takats, J. *Chem. Rev.* **2002**, *102*, 2137.

(8) (a) Kumar, A. S.; Tanase, T.; Iida, M. *Langmuir* **2007**, *23*, 391. (b) Wang, S.; Ferbinteanu, M.; Yamashita, M. *Inorg. Chem.* **2007**, *46*, 610. (c) Hossain, F.; Rigsby, M. A.; Duncan, C. T.; Milligan, P. L., Jr.; Lord, R. L.; Baik, M.-H.; Schultz, F. A *Inorg. Chem.* **2007**, *46*, 2596. (d) Drew, S. C.; Hill, J. P.; Lane, I.; Hanson, G. R.; Gable, R. W.; Young, C. G. *Inorg. Chem.* **2007**, *46*, 2373. (e) Harris, T. D.; Long, J. R. *Chem. Commun.* **2007**, 1360. (f) Lassen, P. R.; Guy, L.; Karame, I.; Roisnel, T.; Vanthuyne, N.; Roussel, C.; Cao, X.; Lombardi, R.; Crassous, J.; Freedman, T. B.; Nafie, L. A. *Inorg. Chem.* **2006**, *45*, 10230. (g) Freedman, D. A.; Kruger, S.; Roosa, C.; Wymer, C. *Inorg. Chem.* **2006**, *45*, 9558. (h) Gu, Z.-G.; Yang, Q.-F.; Liu, W.; Song, Y.; Li, Y.-Z.; Zuo, J.-L.; You, X.-Z. *Inorg. Chem.* **2006**, *45*, 8895. (i) Desrochers, P. J.; Telser, J.; Zvyagin, S. A.; Ozarowski, A.; Krzystek, J.; Vicic, D. A. *Inorg. Chem.* **2006**, *45*, 8930. (j) Wen, H.-R.; Wang, C.-F.; Song, Y.; Gao, S.; Zuo, J.-L.; You, X.-Z. *Inorg. Chem.* **2006**, *45*, 8942. (k) Fructos, M. R.; Trofimenko, S.; Diaz-Requezo, M. M.; Perez, P. J. *J. Am. Chem. Soc.* **2006**, *128*, 11784. (l) Li, D.; Parkin, S.; Clerac, R.; Holmes, S. M. *Inorg. Chem.* **2006**, *45*, 7569. (m) Reger, D. L.; Gardinier, J. R.; Elgin, J. D.; Smith, M. D.; Hautot, D.; Long, G. J.; Grandjean, F. *Inorg. Chem.* **2006**, *45*, 8862. (n) Yamauchi, T.; Takagi, H.; Shibahara, T.; Akashi, H. *Inorg. Chem.* **2006**, *45*, 5429. (o) Dickinson, P. W.; Girolami, G. S. *Inorg. Chem.* **2006**, *45*, 5215.

(9) (a) Trofimenko, S. *Inorg. Chem.* **1969**, *8*, 2675. (b) Byers, P. K.; Canty, A. J.; Honeyman, R. T. *Adv. Organomet. Chem.* **1992**, *34*, 1.

(10) (a) Foley, N. A.; Lail, M.; Lee, J. P.; Gunnoe, T. B.; Cundari, T. R.; Petersen, J. L. *J. Am. Chem. Soc.* **2007**, *129*, 6765. (b) Paneque, M.; Posadas, C. M.; Poveda, M. L.; Rendon, N.; Mereiter, K. *Organometallics* **2007**, *26*, 3120. (c) Vetter, A. J.; Rieth, R. D.; Jones, W. D. *Proc. Natl. Acad. Sci. U.S.A.* **2007**, *104*, 6957. (d) MacDonald, M. G.; Kostelansky, C. N.; White, P. S.; Templeton, J. L. *Organometallics* **2006**, *25*, 4560. (e) Feng, Y.; Gunnoe, T. B.; Grimes, T. V.; Cundari, T. R. *Organometallics* **2006**, *25*, 5456. (f) Braga, A. A. C.; Maseras, F.; Urbano, J.; Caballero, A.; Diaz-Requejo, M. M; Perez, P. J. *Organometallics* **2006**, *25*, 5292. (g) Seidel, W. W.; Schaffrath, M.; Pape, T. *Chem. Commun.* **2006**, 3999. (h) Surendranath, Y.; Welch, K. D.; Nash, B. W.; Harman, W. H.; Myers, W. H.; Harman, W. D. *Organometallics* **2006**, *25*, 5852.

(11) Dhar, S.; Reddy, P. A. N.; Nethaji, M.; Mahadevan, S.; Saha, M. K.; Chakravarty, A. R. *Inorg. Chem.* **2002**, *41*, 3469.

(12) Sigman, D. S. *Acc. Chem. Res.* **1986**, *19*, 180.

(13) Santra, B. K.; Reddy, P. A. N.; Neelakanta, G.; Mahadevan, S.; Nethaji, M.; Chakravarty, A. R. *J. Inorg. Biochem.* **2002**, *89*, 191.

(14) Dhar, S.; Chakravarty, A. R. *Inorg. Chem.* **2005**, *44*, 2582.

(15) (a) Jernigan, F. E.; Sieracki, N. A.; Taylor, M. T.; Jenkins, A. S.; Engel, S. E.; Rowe, B. W.; Jové, F. A.; Yap, G. P. A.; Papish, E. T.; Ferrence, G. M. *Inorg. Chem.* **2007**, *46*, 360. (b) Bigmore, H. R.; Lawrence, S. C.; Mountford, P.; Tredget, C. S. *Dalton Trans.* **2005**, 635. (c) Metcalfe, C.; Adams, H.; Haq, I.; Thomas, J. A. *Chem. Commun.* **2003**, 1152.

(16) Bonnett, R. *Chemical Aspects of Photodynamic Therapy*; Gordon and Breach: London, U.K., 2000.

(17) (a) Henderson, B. W.; Busch, T. M.; Vaughan, L. A.; Frawley, N. P.; Babich, D.; Sosa, T. A.; Zollo, J. D.; Dee, A. S.; Cooper, M. T.; Bellnier, D. A.; Greco, W. R.; Oseroff, A. R. *Cancer Res.* **2000**, *60*, 525. (b) Sternberg, E. D.; Dolphin, D.; Brückner, C. *Tetrahedron* **1998**, *54*, 4151. (c) Ali, H.; van Lier, J. E. *Chem. Rev.* **1999**, *99*, 2379. (d) Magda, D. J.; Wang, Z.; Gerasimchuk, N.; Wei, W.; Anzenbacher, P.; Sessler, J. L. *Pure Appl. Chem.* **2004**, *76*, 365. (e) Clarke, M. J. *Coord. Chem. Rev.* **2003**, *236*, 209. (f) Detty, M. R.; Gibson, S. L.; Wagner, S. J. *J. Med. Chem.* **2004**, *47*, 3897.

(18) (a) Chifotides, H. T.; Dunbar, K. R. *Acc. Chem. Res.* **2005**, *38*, 146. (b) Boerner, L. J. K.; Zaleski, J. M. *Curr. Opin. Chem. Biol.* **2005**, *9*, 135. (c) Erkkila, K. E.; Odom, D. T.; Barton, J. K. *Chem. Rev.* **1999**, *99*, 2777. (d) Armitage, B. *Chem. Rev.* **1998**, *98*, 1171.

(19) (a) Miao, R.; Mongelli, M. T.; Zigler, D. F.; Winkel, B. S. J.; Brewer, K. J. *Inorg. Chem.* **2006**, *45*, 10413. (b) Angeles-Boza, A. M.; Bradley, P. M.; Fu, P. K.-L.; Shatruk, M.; Hilfiger, M. G.; Dunbar, K. R.; Turro, C. *Inorg. Chem.* **2005**, *44*, 7262. (c) Angeles-Boza, A. M.; Bradley, P. M.; Fu, P. K.-L.; Wicke, S. E.; Bacsa, J.; Dunbar, K. R.; Turro, C. *Inorg. Chem.* **2004**, *43*, 8510.

(20) (a) Rajendiran, V.; Karthik, R.; Palaniandavar, M.; Stoeckli-Evans, H.; Periasamy, V. S.; Akbarsha, M. A.; Srinag, B. S.; Krishnamurthy, H. *Inorg. Chem.* **2007**, *46*, 8208. (b) Dhar, S.; Chakravarty, A. R. *Inorg. Chem.* **2003**, *42*, 2483. (c) Dhar, S.; Senapati, D.; Das, P. K.; Chattopadhyay, P.; Nethaji, M.; Chakravarty, A. R. *J. Am. Chem. Soc.* **2003**, *125*, 12112.

(21) (a) Sigman, D. S.; Bruce, T. W.; Sutton, C. L. *Acc. Chem. Res.* **1993**, *26*, 98. (b) Sigman, D. S.; Mazumder, A.; Perrin, D. M. *Chem. Rev.* **1993**, *93*, 2295. (c) Pogozelski, W. K.; Tullius, T. D. *Chem. Rev.* **1998**, *98*, 1089.

(22) Chakravarty, A. R. *J. Chem. Sci.* **2006**, *118*, 443.

(23) Zhang, S. C.; Zhu, Y. G.; Tu, C.; Wei, H. Y.; Yang, Z.; Lin, L. P.; Ding, J.; Zhang, J. F.; Guo, Z. J. *J. Inorg. Biochem.* **2004**, *98*, 2099.

(24) (a) Bales, B. C.; Pitie, M.; Meunier, B.; Greenberg, M. M. *J. Am. Chem. Soc.* **2002**, *124*, 9062. (b) Kurosaki, H.; Maruyama, A.; Koike, H.; Kuroda, N.; Ishikawa, Y.; Goto, M. *Bioorg. Med. Chem. Lett.* **2002**, *12*, 201.

Chart 1. Ternary Complexes $[M(Tp^{Ph})(B)](ClO_4)$ (**1**−**8**) [M = Co(II), Ni(II), Cu(II), Zn(II)] and the Phenanthroline Bases (*B* = 1,10-phenanthroline, dipyridoquinoxaline)

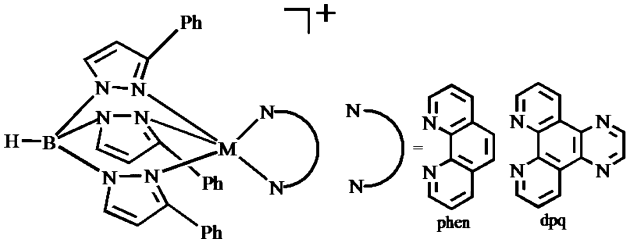

$[M(Tp^{Ph})(phen)](ClO_4)$, M = Co^{II}, 1; Ni^{II}, 2; Cu^{II}, 3; Zn^{II}, 4.
$[M(Tp^{Ph})(dpq)](ClO_4)$, M= Co^{II}, 5; Ni^{II}, 6; Cu^{II}, 7; Zn^{II}, 8.

the complexes. One way to achieve this goal is to use a sterically demanding ligand like Tp^{Ph} that considerably reduces the chemical nuclease activity without affecting the photonuclease activity of the complexes. To explore this possibility, we have extended our study by preparing a series of new complexes of formulation $[M(Tp^{Ph})(B)](ClO_4)$ in addition to the reported Cu(II) complexes, where M = Co(II), Ni(II), Zn(II) and *B* = phen, dpq (Chart 1). Herein, we present the effect of the $\{M(Tp^{Ph})\}$ molecular bowl on the DNA-binding and -cleavage activity of the ternary 3d-metal scorpionates. A preliminary account of this work has earlier been reported.[14]

Experimental Section

Materials. All reagents and chemicals were procured from commercial sources and used as received without further purification. Standard procedures were followed to purify the solvents.[25] Literature procedures were followed to prepare the potassium salt of tris(3-phenylpyrazolyl)borate (KTp^{Ph}) and dipyrido[3,2-d:2′,3′-f]quinoxaline (dpq).[26,27] The complexes $[Cu(Tp^{Ph})(B)](ClO_4)$ (*B* = phen, **3**; dpq, **7**), $[Cu(Tp^{Ph})(dppz)](ClO_4)$, $[Cu(dppz)(NO_3)_2(H_2O)]$, and $[Cu(dpq)(NO_3)(H_2O)_2](NO_3)$ were reported earlier by us.[11,28] Supercoiled (SC) pUC19 DNA (CsCl purified) was purchased from Bangalore Genie (India). Calf thymus (CT) DNA, agarose (molecular biology grade), distamycin-A, superoxide dismutase (SOD), catalase, and ethidium bromide (EB) were purchased from Sigma (USA). Tris(hydroxylmethyl)aminomethane-HCl (Tris-HCl) buffer solution was prepared using deionized sonicated triple distilled water. Tetrabutylammonium perchlorate (TBAP) was used as a supporting electrolyte in the cyclic voltammetric study.

Methods. Elemental analyses were done using a Thermo Finnigan Flash EA 1112 CHNSO analyzer. The infrared, electronic, and emission spectra were recorded on PerkinElmer Lambda 35, PerkinElmer spectrum one 55, and PerkinElmer LS50B spectrophotometers, respectively. Room-temperature magnetic susceptibility data were obtained using Model 300 Lewis-coil-force magnetometer of George Associates Inc. (Berkeley, USA) make. $Hg[Co(NCS)_4]$ was used as a standard. Experimental susceptibility data were corrected for diamagnetic contributions.[29] Molar conductivity measurements were done using a Control Dynamics (India) conductivity meter. Electrospray ionization mass spectral measurements were made using Bruker Daltonics make Esquire 300 Plus ESI Model. Cyclic voltammetric measurements were made at 25 °C on a EG&G PAR Model 253 VersaStat potentiostat/galvanostat with electrochemical analysis software 270 using a three electrode setup consisting of a glassy carbon working, platinum wire auxiliary, and a saturated calomel reference electrode. The electrochemical data were uncorrected for junction potentials.

Preparation of $[M(Tp^{Ph})(B)](ClO_4)$ (M = Co(II), Ni(II), Zn(II); *B* = phen, dpq). The complexes were synthesized by a general procedure in which a suspension of KTp^{Ph} (0.1 g, 0.2 mmol) in 10 mL CH_2Cl_2 was initially stirred for 1 h with a 10 mL CH_2Cl_2 suspension of $[M(H_2O)_6](ClO_4)_2$ (0.2 mmol), followed by an addition of 10 mL CH_2Cl_2 solution of the heterocyclic base (B: 0.04 g phen; 0.05 g dpq; 0.2 mmol) at 0 °C. The reaction mixture was stirred for 30 min, during which a clear solution was obtained. The solution was filtered, and the product was isolated as a solid on slow evaporation of the solvent. The product was purified by washing with a methanol−hexane mixture and dried in vacuum over P_4O_{10}. The yield of the complexes was ∼60%. Single crystals of **4**, **6**, and **8** were grown by slow diffusion of hexane into the CH_2Cl_2 solution of the complexes. Single crystals of **5** were obtained by a diffusion technique using diethyl ether and a MeCN solution of the complex. Anal. Calcd for $C_{39}H_{30}N_8O_4BClCo$ (**1**): C, 60.06; H, 3.88; N, 14.37. Found: C, 59.86; H, 3.75; N, 14.23. ESI-MS in MeCN: *m*/*z* 680 [M^+-ClO_4]. IR (KBr phase, cm^{-1}): 3203br, 2961w, 2924w, 2503m (B−H), 1626s, 1604w, 1585w, 1519m, 1426s, 1346s, 1188m, 1108vs (ClO_4^-), 843m, 795m, 761s, 694m, 623m (vs, very strong; s, strong; m, medium; w, weak; br, broad). UV−vis in DMF-Tris-HCl buffer (2:1 v/v) [λ_{max}/nm (ε/ M^{-1} cm^{-1})]: 507sh (70), 267 (40 200) (sh, shoulder). Λ_M (S m^2 M^{-1}) in DMF at 25 °C: 68. μ_{eff} = 4.11 μ_B at 298 K. Anal. Calcd for $C_{39}H_{30}N_8O_4BClNi$ (**2**): C, 60.08; H, 3.88; N, 14.37. Found C, 59.87; H, 3.78; N, 14.42. ESI-MS in MeCN: *m*/*z* 679.2 [M^+-ClO_4]. IR (KBr phase, cm^{-1}): 3207br, 2940w, 2490m (B−H), 1630s, 1600w, 1570w, 1510m, 1420s, 1326s, 1190m, 1100vs (ClO_4^-), 850m, 795m, 680m, 630m. UV−vis in DMF-Tris-HCl buffer (2:1 v/v) [λ_{max}/nm (ε/ M^{-1} cm^{-1})]: 640 (10), 265 (38 300). Molar conductivity (Λ_M, S m^2 M^{-1}) in DMF at 25 °C: 66. μ_{eff} = 2.91 μ_B at 298 K. Anal. Calcd for $C_{39}H_{30}N_8O_4BClZn$ (**4**): C, 59.57; H, 3.85; N, 14.25. Found: C, 59.59; H, 3.80; N, 14.12. ESI-MS in MeCN: *m*/*z* 685 [M^+-ClO_4]. IR (KBr phase, cm^{-1}): 3401br, 3140m, 3066m, 2528m (B−H), 1606m, 1583m, 1521m, 1469s, 1428s, 1359s, 1191s, 1099vs (ClO_4^-), 842m, 805m, 769s, 700m. UV−vis in DMF-Tris-HCl buffer (2:1 v/v) [λ_{max}/nm (ε/ M^{-1} cm^{-1})]: 265 (65 700). Λ_M (S m^2 M^{-1}) in DMF at 25 °C: 66. Anal. Calcd for $C_{41}H_{30}N_{10}O_4BClCo$ (**5**): C, 59.19; H, 3.63; N 16.84. Found: C, 59.34; H, 3.68; N, 16.76. ESI-MS in MeCN: *m*/*z* 732 [M^+-ClO_4]. IR (KBr phase, cm^{-1}): 3450br, 2964w, 2495m (B−H), 1580w, 1524w, 1489w, 1489s, 1467s, 1406w, 1388w, 1356m, 1307s, 1190s, 1098vs (ClO_4^-), 956w, 841w, 760s, 694s, 621m. UV−vis in DMF-Tris-HCl buffer (2:1 v/v) [λ_{max}/nm (ε/ M^{-1} cm^{-1})]: 518sh (105), 345 (3820), 269 (65 100). Λ_M (S m^2 M^{-1}) in DMF at 25 °C: 72. μ_{eff} = 4.29 μ_B at 298 K. Anal. Calcd for $C_{41}H_{30}N_{10}O_4BClNi$ (**6**): C, 59.21; H, 3.64; N, 16.84. Found: C, 59.34; H, 3.54; N, 16.68. ESI-MS in MeCN: *m*/*z* 731 [M^+-ClO_4]. IR (KBr phase, cm^{-1}): 3351br, 2962s, 2477m (B−H), 1952s, 1581m, 1523m, 1490s, 1467s, 1404w, 1388w, 1306s, 1190m, 1095vs (ClO_4^-), 838s, 763s, 694s, 621m. UV−vis in DMF-Tris-HCl buffer (2:1 v/v) [λ_{max}/nm (ε/M^{-1} cm^{-1})]: 598 (15), 340 (2100), 323 (3200), 263 (52 100). Λ_M (S m^2 M^{-1}) in DMF at 25 °C: 75. μ_{eff} = 2.93 μ_B at 298 K. Anal. Calcd for $C_{41}H_{30}N_{10}O_4BClZn$ (**8**): C, 58.74; H, 3.61; N, 16.71. Found: C, 59.02; H, 3.72; N, 16.58. ESI-MS in MeCN: *m*/*z* 737.3 [M^+-ClO_4].

(25) Perrin, D. D.; Armarego, W. L. F.; Perrin, D. R. *Purification of Laboratory Chemicals*; Pergamon Press: Oxford, 1980.
(26) Eichhorn, D. M.; Armstrong, W. H. *Inorg. Chem.* **1990**, *29*, 3607.
(27) Collins, J. G.; Sleeman, A. D.; Aldrich-Wright, J. R.; Greguric, I.; Hambly, T. W. *Inorg. Chem.* **1998**, *37*, 3133.
(28) Thomas, A. M.; Nethaji, M.; Mahadevan, S.; Chakravarty, A. R. *J. Inorg. Biochem.* **2003**, *94*, 171.
(29) Khan, O. *Molecular Magnetism*; VCH: Weinheim, 1993.

IR (KBr phase, cm^{-1}): 3540br, 2962w, 2483m (B−H), 1581m, 1523m, 1490s, 1468s, 1388m, 1360s, 1098vs (ClO_4^-), 763s, 698s, 623s. UV−vis in DMF-Tris-HCl buffer (2:1 v/v) [λ_{max}/nm (ε/M^{-1} cm^{-1})]: 340 (3400), 327 (4200), 267 (36800). Λ_M (S m^2 M^{-1}) in DMF at 25 °C: 75.

Solubility and Stability. The complexes showed good solubility in CH_2Cl_2, MeCN, MeOH, DMSO, and DMF and low solubility in aqueous medium. Perchlorate salts of the metal complexes being potentially explosive, samples with only small quantity were used with necessary precautions. The ternary complexes were found to be stable in solution and solid state. The significant peaks in the mass spectra of the complexes corresponded to the complex ion peaks, suggesting the stability of the ternary structures in the solution phase (Figures S1−S6 in the Supporting Information).

X-ray Crystallographic Procedures. The crystal structures of **4**−**6** and **8** were obtained by single-crystal X-ray diffraction technique. Crystal mounting was done on glass fiber with epoxy cement. All geometric and intensity data were collected at room temperature using an automated Bruker SMART APEX CCD diffractometer equipped with a fine focus 1.75 kW sealed tube Mo Kα X-ray source (λ = 0.71073 Å) with increasing ω (width of 0.3° per frame) at a scan speed of 8, 5, 10, and 8 s per frame for **4**−**6** and **8**, respectively. Intensity data, collected using ω-2θ scan-modes, were corrected for Lorentz-polarization effects. Empirical absorption corrections were made using the *SADABS* program.[30] Structures were solved by the combination of Patterson and Fourier techniques and refined by full-matrix least-squares method using the *SHELX* system of programs.[31] All hydrogen atoms belonging to the complexes were fixed in their calculated positions and refined using a riding model. All non-hydrogen atoms were refined anisotropically. The perspective views of the complexes were obtained using the *ORTEP* program.[32] Unit cell packing diagrams are given as Supporting Information (Figures S7−S10).

DNA-Binding Experiments. The experiments involving the interaction of the complexes with calf thymus (CT) DNA were carried out in Tris-HCl buffer (5 mM Tris-HCl, pH 7.2) containing 5% DMF at room temperature. Thermal denaturation studies were carried out in melting-buffer (5 mM Na_2HPO_4, 5 mM NaH_2PO_4, 1 mM Na_2EDTA and 5 mM NaCl). A solution of calf thymus DNA in the buffer gave a ratio of UV absorbance at 260 and 280 nm of about 1.9:1, indicating that the DNA was sufficiently free from protein.[33] The concentration of CT DNA was measured from its absorption intensity at 260 nm using the molar absorption coefficient value of 6600 M^{-1} cm^{-1}.[34] In absorption titration experiments, the concentration of the CT DNA was varied keeping the complex concentration as constant (25 and 50 μM). Due correction was made for the absorbance of DNA itself. The spectra were recorded after equilibration for 5 min. The intrinsic equilibrium binding constants (K_b) of the complexes to CT DNA were obtained using the McGhee−von Hippel (MvH) method using the expression of Bard and co-workers by monitoring the change in the absorption intensity of the charge-transfer spectral band at ∼265 nm with increasing concentration of CT DNA by regression analysis using eq (1),

$$(\varepsilon_a - \varepsilon_f)/(\varepsilon_b - \varepsilon_f) = (b - (b^2 - 2K_bC_t[DNA]/s)^{1/2})/2K_bC_t$$
$$b = 1 + K_bC_t + K_b[DNA]/2s \quad (1)$$

where ε_a is the extinction coefficient observed for the charge transfer absorption band at a given DNA concentration, ε_f is the extinction coefficient of the complex free in solution, ε_b is the extinction coefficient of the complex when fully bound to DNA, K_b is the equilibrium binding constant, C_t is the total complex concentration, [DNA] is the DNA concentration in nucleotides, and s is the binding site size in base pairs (Figure S11 in the Supporting Information).[35,36] The nonlinear least-squares analysis was done using *Origin Laboratory*, version 6.1.

DNA melting experiments were carried out by monitoring the absorption intensity of CT DNA (200 μM) at 260 nm at various temperatures, both in the absence and presence of the metal scorpionates (100 μM). Measurements were carried out using a PerkinElmer Lambda 35 spectrophotometer equipped with a Peltier temperature-controlling programmer (PTP 6) (±0.1 °C) on increasing the temperature of the solution at 0.25 °C per min (Figures S12, S13 in the Supporting Information). Viscometric titrations were performed using Schott Gerate AVS 310 Automated Viscometer that was thermostatted at 37 ± 0.1 °C in a constant temperature bath. The concentration of CT DNA was 135 μM in NP, and the flow times were measured with an automated timer. Each sample was measured 3 times and an average flow time was calculated. Data were presented as $(\eta/\eta_0)^{1/3}$ versus [complex]/[DNA], where η is the viscosity of DNA in the presence of the complex and η_0 is that of DNA alone (Figure S14 in the Supporting Information).[37] Viscosity values were calculated from the observed flowing time of DNA-containing solutions (t) corrected for that of buffer alone (t_0), $\eta = (t - t_0)$. The relative binding propensity of the ternary complexes to CT DNA was studied by the fluorescence spectral method using EB-bound CT DNA solution in Tris-HCl/NaCl buffer (pH 7.2) (Figure S15 in the Supporting Information). The apparent binding constant (K_{app}) was calculated from the equation: $K_{EB} \times [EB] = K_{app} \times [complex]$, where [complex] is the concentration of the complex at 50% reduction of the fluorescence intensity, $K_{EB} = 1.0 \times 10^7$ M^{-1} and [EB] = 1.3 μM.[38]

DNA Cleavage Experiments. The chemical nuclease activity of the complexes was studied using supercoiled (SC) pUC19 DNA in a medium of Tris-HCl/NaCl buffer using 3-mercaptopropionic acid (MPA) as a reducing agent and hydrogen peroxide (H_2O_2) as an oxidizing agent. The cleavage of SC DNA (30 μM, 0.2 μg, 2686 base-pair) was studied by agarose gel electrophoresis using metal complexes in 50 mM Tris-HCl buffer (pH 7.2) containing 10% DMF and 50 mM NaCl. For photoinduced DNA-cleavage studies, the reactions were carried out under illuminated conditions using a UV-A source at 365 nm (12 W, Bangalore Genie make) and a visible laser light source (Spectra Physics Water-Cooled Mixed-Gas Ion Laser Stabilite 2018-RM with beam diameter at $1/e^2$ 1.8 mm ± 10% and beam divergence with a full angle of 0.70 mrad ± 10%). The sample with a solution path-length of 5 mm was positioned at a distance of 10 cm from the aperture of the laser. The power of the laser beam was measured using a Spectra Physics CW Laser Power Meter (Model 407A) at the sample position. After exposure to the light, each sample was incubated for 1.0 h at 37 °C and analyzed for the photocleaved products, using gel electro-

(30) Walker, N.; Stuart, D. *Acta Crystallogr.* **1983**, *A39*, 158.
(31) Sheldrick, G. M. *SHELX-97, Programs for Crystal Structure Solution and Refinement*; University of Göttingen: Göttingen, Germany.
(32) Johnson, C. K. *ORTEP-III, Report ORNL-5138*; Oak Ridge National Laboratory: Oak Ridge, TN, 1976.
(33) Merill, C.; Goldman, D.; Sedman, S. A.; Ebert, M. H. *Science* **1980**, *211*, 1437.
(34) Reichman, M. E.; Rice, S. A.; Thomas, C. A.; Doty, P. *J. Am. Chem. Soc.* **1954**, *76*, 3047.
(35) McGhee, J. D.; von Hippel, P. H. *J. Mol. Biol.* **1974**, *86*, 469.
(36) Carter, M. T.; Rodriguez, M.; Bard, A. J. *J. Am. Chem. Soc.* **1989**, *111*, 8901.
(37) Satyanarayana, S.; Dabrowiak, J. C.; Chaires, J. B. *Biochemistry* **1992**, *31*, 9319.
(38) Lee, M.; Rhodes, A. L.; Wyatt, M. D.; Forrow, S.; Hartley, J. A. *Biochemistry* **1993**, *32*, 4237.

Table 1. Selected Physicochemical Data and DNA-Binding Parameters for the Complexes **1**−**8**

complex	λ, nm (ε, M^{-1} cm^{-1})[a]	μ_{eff},[b]/BM	$10^{-4}K_b/M^{-1}$, [s/bp][c]	$10^{-5}K_{app}$[d]/M^{-1}	ΔT_m[e]/°C
[Co(Tp^{Ph})(phen)](ClO$_4$) (**1**)	507 (70)	4.11	1.2 ± 0.2[0.1]	1.1 ± 0.1	1.4
[Ni(Tp^{Ph})(phen)](ClO$_4$) (**2**)	640 (10)	2.91	2.7 ± 0.4[0.2]	1.6 ± 0.2	1.2
[Cu(Tp^{Ph})(phen)](ClO$_4$) (**3**)[f]	660 (74)	1.75	1.0 ± 0.1[0.4]	1.0 ± 0.1	1.6
[Zn(Tp^{Ph})(phen)](ClO$_4$) (**4**)[g]			2.2 ± 0.1[0.3]	1.4 ± 0.2	1.3
[Co(Tp^{Ph})(dpq)](ClO$_4$) (**5**)	518 (105)	4.29	5.9 ± 0.1[0.3]	2.8 ± 0.1	2.1
[Ni(Tp^{Ph})(dpq)](ClO$_4$) (**6**)	598 (15)	2.93	9.1 ± 0.2[0.4]	3.8 ± 0.1	1.8
[Cu(Tp^{Ph})(dpq)](ClO$_4$) (**7**)[f]	643 (80)	1.78	7.5 ± 0.3[0.5]	3.5 ± 0.1	2.2
[Zn(Tp^{Ph})(dpq)](ClO$_4$) (**8**)[g]			8.1 ± 0.3[0.3]	3.4 ± 0.2	2.3

[a] Visible electronic spectral band in DMF-Tris buffer. [b] μ_{eff} in μ_B for solid powdered samples at 298 K. [c] Intrinsic DNA-binding constant (*s*, binding site size). [d] Apparent DNA-binding constant by emission spectral method. [e] Change in DNA melting temperature. [f] Refs 11 and 14. [g] Diamagnetic.

Table 2. Selected Crystallographic Data for **4**−**6** and **8**

	[Zn(Tp^{Ph})(phen)](ClO$_4$) (**4**)	[Co(Tp^{Ph})(dpq)](ClO$_4$)·Et$_2$O (**5**·Et$_2$O)	[Ni(Tp^{Ph})(dpq)](ClO$_4$)·2H$_2$O (**6**·2H$_2$O)	[Zn(Tp^{Ph})(dpq)](ClO$_4$)·2H$_2$O (**8**·2H$_2$O)
formula	$C_{39}H_{30}BClN_8O_4Zn$	$C_{45}H_{40}BClCoN_{10}O_5$	$C_{41}H_{34}BClN_{10}NiO_6$	$C_{41}H_{34}BClN_{10}O_6Zn$
fw, g M^{-1}	786.34	906.06	867.75	874.41
cryst syst	monoclinic	monoclinic	monoclinic	monoclinic
space group (no.)	$P2_1/n$ (14)	Cc (9)	Cc (9)	Cc (9)
a, Å	15.437(5)	22.1054(16)	22.250(11)	22.148(7)
b, Å	17.368(5)	13.4737(10)	13.366(6)	13.415(4)
c, Å	15.690(5)	14.5452(11)	14.372(7)	14.454(5)
β, deg	119.197(6)	101.014(1)	100.590(8)	101.029(6)
V, Å^3	3672.1(19)	4252.4(5)	4201(4)	4215(2)
Z	4	4	4	4
T, K	293(2)	293(2)	293(2)	293(2)
ρ_{calcd}, g cm^{-3}	1.422	1.415	1.372	1.378
λ, Å Mo Kα	0.71073	0.71073	0.71073	0.71073
μ, mm^{-1}	0.795	0.526	0.584	0.705
data/restraints/params	6405/0/487	7904/2/568	7959/2/541	7961/2/541
GOF on F^2	1.292	1.035	1.069	1.078
R(F_o)[a] [wR(F_o)][b] [$I > 2\sigma(I)$]	0.1159 [0.2119]	0.0473 [0.1027]	0.0677 [0.1597]	0.0716 [0.1577]
R (wR) [all data]	0.1420 (0.2231)	0.0651 (0.1119)	0.0864 (0.1717)	0.0934 (0.1692)
largest diff. peak and hole (e·Å^{-3})	0.769, −0.634	0.362, −0.251	0.714, −0.652	0.782, −0.322
$w = 1/[\sigma^2(F_o^2) + (AP)^2 + (BP)]$	$A = 0.0701$; $B = 7.6996$	A = 0.0574; B = 0.0000	A = 0.0987; $B = 0.0000$	A = 0.0868; $B = 0.0000$

[a] $R = \Sigma||F_o| - |F_c||/\Sigma|F_o|$. [b] $wR = \{\Sigma[w(F_o^2 - F_c^2)^2]/\Sigma[w(F_o^2)^2]\}^{1/2}$; $w = [\sigma^2(F_o)^2 + (AP)^2 + BP]^{-1}$, where $P = (F_o^2 + 2F_c^2)/3$.

phoresis as discussed below. The inhibition reactions for the photoinduced DNA cleavage were carried out at 365 nm using different reagents (NaN_3, 200 μM; DMSO, 3 μL; catalase, 4 units; SOD, 4 units; distamycin-A, 20 μM) prior to the addition of the complex. For the D_2O experiment, this solvent was used for dilution of the sample to 20 μL. The samples after incubation for 1.0 h at 37 °C in a dark chamber were added to the loading buffer containing 25% bromophenol blue, 0.25% xylene cyanol, 30% glycerol (3 μL), and the solution was finally loaded on 1.0% agarose gel containing 1.0 μg/mL EB. Electrophoresis was carried out in a dark chamber for 2.0 h at 60 V in TAE (Tris-acetate EDTA) buffer. Bands were visualized by UV light and photographed. The extent of DNA cleavage was measured from the intensities of the bands using the UVITEC Gel Documentation System. Due corrections were made for the low level of nicked circular (NC) form present in the original supercoiled (SC) DNA sample and for the low affinity of EB binding to SC compared to NC and linear forms of DNA.[39] The concentrations of the complexes and reagents corresponded to the quantity of the sample after dilution to the 20 μL final volume with Tris-HCl buffer. The observed error in measuring the band intensities ranged between 3−7%.

Results and Discussion

Synthesis and General Aspects. The bivalent 3d-metal complexes of formulation [M(Tp^{Ph})(B)](ClO$_4$) (**1**−**8**) were synthesized in high yield from a reaction of [M(H$_2$O)$_6$](ClO$_4$)$_2$ with the potassium salt of tris(3-phenylpyrazolyl)borate (KTp^{Ph}) and the heterocyclic base (B) and isolated as perchlorate salts (Chart 1). Characterization of the complexes was done from their analytical and physicochemical data (Table 1). The 1:1 electrolytic complexes showed the presence of characteristic ClO_4^- and B−H infrared bands at ∼1090 and ∼2500 cm^{-1}, respectively.[11] The complexes except the Zn(II) species exhibited visible spectral band in the electronic spectra in DMF-Tris buffer (Figures S16, S17). The ligand based electronic spectral bands were observed in the UV range. The complexes did not show any metal-based redox process except the Cu(II) complexes. The redox chemistry of the Cu(II) complexes **3** and **7** showing quasi-reversible cyclic voltammetric response near 0.0 V vs SCE with an i_{pc}/i_{pa} peak-current ratio of unity in DMF-0.1 M TBAP was reported earlier.[11]

4−**6** and **8** were structurally characterized by the X-ray diffraction technique. The crystal structures of **3** and **7** are known.[11] Selected crystal data are given in Table 2. The bond distances and angles are given as Supporting Information (Tables S1−S4). Perspective views of the complexes are shown in Figures 1 and 2. The structures of the cationic complexes are essentially similar.[11] The complexes are discrete monomeric species with the metal in a distorted

(39) Bernadou, J.; Pratviel, G.; Bennis, F.; Girardet, M.; Meunier, B. *Biochemistry* **1989**, *28*, 7268.

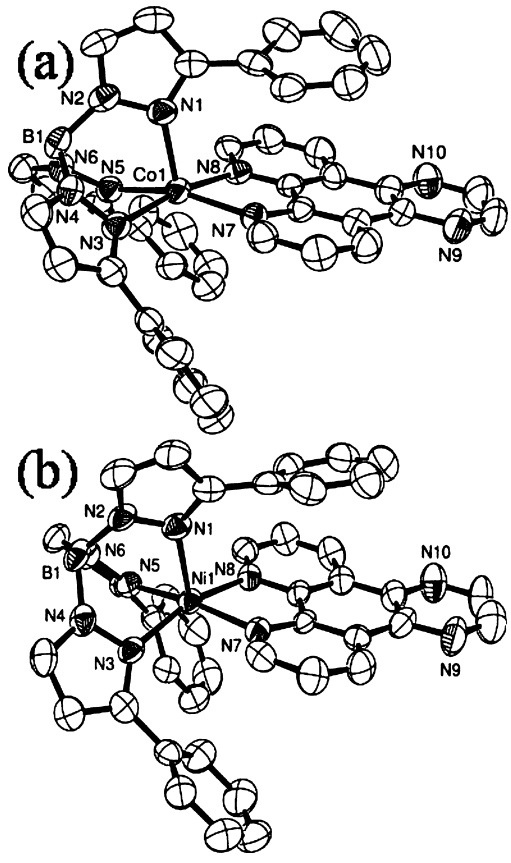

Figure 1. ORTEP views of the cationic complexes of $[Co(Tp^{Ph})(dpq)](ClO_4)\cdot Et_2O$ (**5**·Et_2O) (a) and $[Ni(Tp^{Ph})(dpq)](ClO_4)\cdot 2H_2O$ (**6**·$2H_2O$) (b) showing 50% probability thermal ellipsoids and the atom numbering scheme for the metal and hetero atoms.

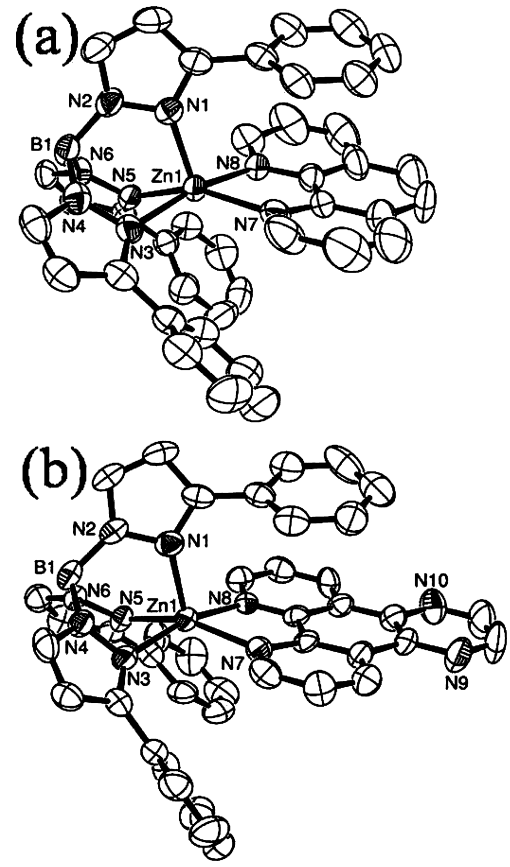

Figure 2. ORTEP views of the cationic complexes of $[Zn(Tp^{Ph})(phen)](ClO_4)$ (**4**) (a) and $[Zn(Tp^{Ph})(dpq)](ClO_4)\cdot 2H_2O$ (**8**·$2H_2O$) (b) with 50% probability thermal ellipsoids and the atom numbering scheme for the metal and hetero atoms.

square-pyramidal coordination geometry. The trigonal distortion parameter (τ) values for **4**−**6** and **8** are 0.26, 0.13, 0.10, and 0.13, respectively.[40] The donor atoms in the basal plane are two nitrogen atoms from the heterocyclic base B and two nitrogen atoms of the Tp^{Ph} ligand. The nitrogen atom of the third 3-phenylpyrazolyl is bonded at the apical site. The M−N equatorial and axial distances are 2.1 and 2.0 Å, respectively. Three phenyl groups of the Tp^{Ph} anion form a bowl shaped structure that sterically encloses the $\{M^{II}(B)\}$ moiety. The steric effect is visible for both the phen and dpq complexes. The Tp^{Ph} ligand provides a hydrophobic environment to the photoactive quinoxaline moiety of the dpq ligand, thus making it inaccessible to the solvent molecules.

DNA Binding Studies. The binding propensity of the ternary 3d-metal complexes to calf thymus (CT) DNA was studied using various techniques. The DNA-binding parameters are given in Table 1. Electronic spectral titrations were carried out to determine the intrinsic equilibrium binding constant (K_b) along with the binding site size(s) of the complexes bound to CT-DNA by monitoring the change in the absorption intensity of the ligand centered bands (part a of Figure 3). A complex generally shows hypochromism and red shift (bathochromism) of the absorption band when it binds to DNA through intercalation resulting strong stacking interaction between the aromatic chromophore of the ligand and the base pairs of the double strand (ds) DNA.[41] The extent of hypochromism gives a measure of the strength of an intercalative binding. The present complexes show 40−60% of hypochromism upon binding to CT-DNA. The observed hypochromism and K_b values among the present complexes follow the order: dpq complexes (**5**−**8**) > phen complexes (**1**−**4**). The intrinsic equilibrium DNA-binding constant values for **1**−**4** (phen) and **5**−**8** (dpq) are in the range of 1.0×10^4 to 2.7×10^4 and 5.9×10^4 to 9.1×10^4 M^{-1}, respectively. The poor DNA-binding propensity of the complexes could be due to the presence of Tp^{Ph} as a steric protector ligand.

Thermal denaturation, emission spectral, and viscosity measurements were done to get further insights into the DNA-binding nature of the complexes. In thermal denaturation study, an increase of temperature tends to gradually dissociate the double-strand (ds) DNA to single strands. We have observed only a minor increase (1−3 °C) in the DNA melting temperature of CT-DNA in the presence of **1**−**8**, indicating the groove and/or electrostatic binding nature of the complexes. Viscosity measurements on the solutions of CT DNA incubated with the complexes were carried out to determine the relative specific viscosity (η/η_0) of CT DNA.

(40) Addison, A. W.; Rao, T. N.; Reedijk, J. V.; van Rijn, J.; Verschoor, G. C. *J. Chem. Soc., Dalton Trans.* **1984**, 1349.

(41) (a) Bilakhiya, A. K.; Tyagi, B.; Paul, P.; Natarajan, P. *Inorg. Chem.* **2002**, *41*, 3830. (b) Tysoe, S. A.; Morgan, R. J.; Baker, A. D.; Strekas, T. C. *J. Phys. Chem.* **1993**, *97*, 1707.

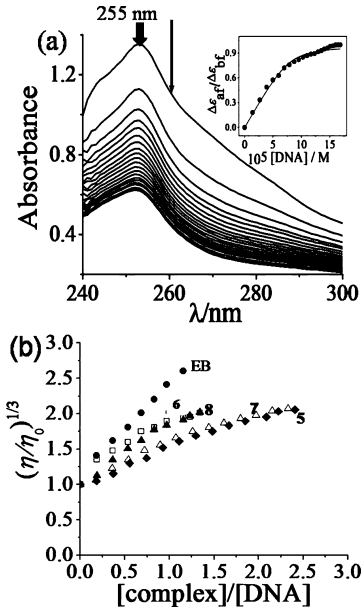

Figure 3. (a) Absorption spectral traces of **7** on increasing concentration of CT-DNA with the inset showing least-squares fit of $\Delta\varepsilon_{af}/\Delta\varepsilon_{bf}$ vs [DNA] using the MvH equation. (b) Effect of increasing the quantity of {Tp^{Ph}−M(II)−dpq} [**5** (◆), **6** (□), 7 (Δ), 8 (▲)] on the relative viscosities of CT-DNA at 37.0 (±0.1) °C in 5 mM Tris-HCl buffer (pH 7.2) ([DNA] = 165 μM). The viscosity data for ethidium bromide (EB, ●) in water are also shown for comparison.

Because the η/η_0 of DNA gives a measure on the increase in contour length associated with the separation of DNA base pairs caused by intercalation, a classical DNA intercalator like ethidium bromide (EB) shows a significant increase in the viscosity of the DNA solutions, where η and η_0 are the specific viscosities of DNA in the presence and absence of the complexes, respectively. In contrast, a partial and/or non-intercalation of the ligand could result in less pronounced effect on the viscosity.[42] The relative viscosity of DNA was found to increase marginally on increasing the concentration of the complexes. The plot of relative specific viscosity $(\eta/\eta_0)^{1/3}$ versus [complex]/[DNA] ratio for **5**−**8** shows only minor change in the viscosity in comparison to that of the DNA intercalating EB (part b of Figure 3). The relative viscosity of DNA and contour length follows the equation: $(\eta/\eta_0) = (L/L_0)^{1/3}$, where L and L_0 are the contour lengths of DNA in the presence and absence of the complexes, respectively.[37] The change in relative viscosity for the dpq complexes is more than those for the phen analogues, suggesting greater DNA-binding propensity of the dpq complexes. The viscosity results suggest primarily DNA-groove and/or surface-binding nature of the complexes.

The emission spectral method was used to get an estimate on the relative binding of the complexes to CT-DNA. EB was used as a spectral probe as it shows no apparent emission intensity in the buffer solution because of solvent quenching and an enhancement of the emission intensity when it intercalates to DNA.[38,43] The reduction of the emission intensity of EB on increasing the complex concentration could have resulted from the displacement of the DNA-bound EB by the ternary metal scorpionates or quenching by the paramagnetic complexes bound to DNA (Figure S15 in the Supporting Information). Addition of the complexes to DNA was found to decrease the emission intensity of EB. Because the paramagnetic Co(II), Ni(II), Cu(II), and diamagnetic Zn(II) complexes showed similar K_{app} values, the displacement of EB by the complexes could be more probable than the paramagnetic quenching. The apparent binding constant (K_{app}) values of the complexes to DNA, measured from the extent of the reduction of the emission intensity, were $\sim 10^5$ M^{-1}. The dpq complexes showed higher K_{app} values than the phen analogues.

Table 3. Selected Photo-Induced SC pUC19 DNA (0.2 μg, 30 μM) Cleavage Data of **1**−**8** on Irradiation with UV-A and Visible Light for an Exposure Time of 2 h

Sl. No.	reaction condition	%NC λ = 365 nm[a]	%NC λ = 514.5 nm[b]	%NC λ = 647.1 nm[a]
1	DNA control	3	4	4
2	DNA + dpq (10 μM)	10	9	
3	DNA + **1**	8	12	
4	DNA + **2**	10	13	
5	DNA + **3**	42		
6	DNA + **4**	6	14	
7	DNA + **5**	85	65	
8	DNA + **6**	45	11	
9	DNA + **7**	99		80
10	DNA + [Cu(Tp^{Ph})(dppz)](ClO_4)[a]			82
11	DNA + **8**	57	12	
12	DNA + **7**[c]	49[c]		
13	DNA + [Cu(dpq)(NO_3)(H_2O)$_2$](NO_3)[c]	23[c]		

[a] [complex] = 10 μM. [b] [complex] = 60 μM. [c] [complex] = 2.5 μM, exposure time = 30 min.

Chemical Nuclease Activity. Redox-active complexes are expected to show good chemical nuclease activity in the presence of metal-based redox couple(s). For example, redox-active Cu(II) complexes having a readily accessible Cu(II)/Cu(I) couple show efficient chemical nuclease activity in the presence of a reducing agent like ascorbic acid or 3-mercaptopropionic acid (MPA).[44] In contrast, the present bivalent 3d-metal complexes, in the absence of any metal-based redox couple, do not show any significant chemical nuclease activity for the Co(II), Ni(II), and Zn(II) ions on addition of MPA. The Cu(II) complexes **3** and **7** are also poor cleavers of supercoiled (SC) pUC19 DNA in the presence of MPA, whereas $[Cu(phen)_2]^{2+}$ (5 μM), used as a control, shows efficient DNA cleavage under similar reaction conditions (Figure S18 in the Supporting Information).[11] The steric enclosure of the DNA-binding phenanthroline bases by Tp^{Ph} could be the reason for the poor chemical nuclease activity of the complexes. The Co(II) complexes do not show any significant chemical nuclease activity on addition of H_2O_2 as an oxidizing agent.

DNA-Photocleavage Activity. The photoinduced DNA-cleavage activity of the complexes were studied using SC pUC19 DNA in a medium of Tris-HCl/NaCl buffer on

(42) (a) Gabbay, E. J.; Scofield, R. E.; Baxter, C. S. *J. Am. Chem. Soc.* **1973**, *95*, 7850. (b) Veal, J. M.; Rill, R. L. *Biochemistry* **1991**, *30*, 1132.

(43) (a) Waring, M. J. *J. Mol. Biol.* **1965**, *13*, 269. (b) LePecq, J.-B.; Paoletti, C. *J. Mol. Biol.* **1967**, *27*, 87.

(44) (a) Mahadevan, S.; Palaniandavar, M. *Inorg. Chem.* **1998**, *37*, 693. (b) Patra, A. K.; Dhar, S.; Nethaji, M.; Chakravarty, A. R. *Dalton Trans.* **2005**, 896. (c) Patra, A. K.; Nethaji, M.; Chakravarty, A. R. *Dalton Trans.* **2005**, 2798.

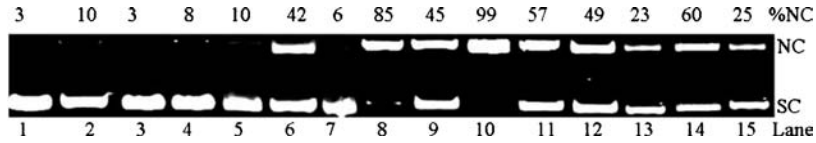

Figure 4. Cleavage of SC pUC19 DNA (0.2 μg, 30 μM) by **1**−**8**, [Cu(dppz)$(NO_3)_2(H_2O)$], and [Cu(dpq)$(NO_3)(H_2O)_2](NO_3)$ in 50 mM Tris-HCl/NaCl buffer (pH, 7.2) containing 10% DMF on photoirradiation at 365 nm (12 W): lane 1, DNA control (t = 2 h); lane 2, DNA + dpq (10 μM, t = 2 h)); lane 3, DNA + KTp^{Ph} (10 μM, t = 2 h); lanes 4−11, DNA + **1**−**8** (10 μM, t = 2 h); lane 12, DNA + **7** (2.5 μM, t = 30 min); lane 13, [Cu(dpq)$(NO_3)(H_2O)_2](NO_3)$ (2.5 μM, t = 30 min); lane 14, [Cu(Tp^{Ph})(dppz)](ClO_4) (2.5 μM, t = 30 min); lane 15, [Cu(dppz)$(NO_3)_2(H_2O)$] (2.5 μM, t = 30 min).

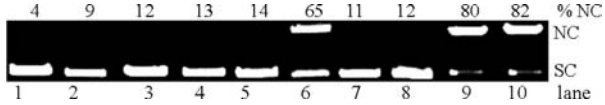

Figure 5. Cleavage of SC pUC19 DNA (0.2 μg, 30 μM) by **1**−**8** and [Cu(Tp^{Ph})(dppz)](ClO_4) in visible light of 514 nm (200 mW, 60 μM, lanes 1−8) and at 647.1 nm (100 mW, lanes 9 and 10) for an exposure time of 2 h: lane 1, DNA control; lane 2, DNA + dpq (60 μM); lane 3, DNA + **1**; lane 4, DNA + **2**; lanes 5−7, DNA + **4**−**6**; lane 8, DNA + **8**; lane 9, DNA + **7** (10 μM); lane 10, DNA + [Cu(Tp^{Ph})(dppz)](ClO_4)(10 μM).

irradiation with monochromatic UV-A light of 365 nm (12 W) and in visible light with a tunable multicolor Ar−Kr mixed gas ion laser (Table 3; Figures 4, 5; and Figures S19−S23 in the Supporting Infomation). It has been observed that both the complexes [Cu(Tp^{Ph})(dpq)](ClO_4)[14] and [Co(Tp^{Ph})-(dpq)](ClO_4) are efficient cleavers of SC DNA in UV-A and visible light. Whereas phen **1**−**4** are poor photocleavers of DNA, the dpq analogues **5**−**8** showed efficient photoinduced DNA-cleavage activity in UV-A light. The quinoxaline moiety of dpq could generate the photoexcited $^3(n\text{-}\pi^*)$ and/or $^3(\pi\text{-}\pi^*)$ states, causing the cleavage of DNA as observed for the quinoxaline antibiotics.[45] A 10 μM solution of the dpq complex of Co(II) (**5**) on irradiation at 365 nm for 2 h showed significant cleavage (∼85%) of SC DNA to its nicked circular (NC) form (Lane 8, Figure 4). The Ni(II) and Zn(II) complexes (**6** and **8**) showed ∼50% conversion of SC DNA to its NC form (Lanes 9 and 11, Figure 4). The Cu(II) complex (**7**) showed essentially complete cleavage of DNA (99%) under similar reaction conditions (Lane 10, Figure 4).

The effect of steric protection of the photosensitizer by the Tp^{Ph} ligand in **5**−**8** was investigated using [Cu(dpq)-$(NO_3)(H_2O)_2](NO_3)$ as a control agent.[28] A 2.5 μM complex **7** showed better cleavage activity than [Cu(dpq)(NO_3)-$(H_2O)_2](NO_3)$ in UV-A light of 365 nm (Figure 4). Similarly, $[Cu(Tp^{Ph})(dppz)]^+$ was found to be more efficient photocleaver of DNA than [Cu(dppz)$(NO_3)_2(H_2O)$] (Figure 4).[14,28] The results indicate that the sterically protected dpq or dppz ligand is a better photosensitizer than the unprotected one. Among the four $\{Tp^{Ph}\text{-M(II)-dpq}\}^+$ complexes, only Co(II) (**5**) and Cu(II) (**7**) are efficient photocleavers of DNA in visible light.[46,47] A 60 μM solution of **5** on irradiation at 514 nm for 2 h exhibited ∼65% cleavage of SC DNA, whereas its Cu(II) analogue at 647.1 nm displayed ∼80% DNA cleavage (Lanes 6 and 9, Figure 5). $[Ni(Tp^{Ph})(dpq)]^+$ is a poor cleaver of DNA in visible light.[46] This could be possibly due to a very low molar extinction coefficient value of the visible electronic band for Ni(II), thus making any metal-assisted photosensitization process unfavorable.[20c] The d^{10}−Zn(II) complex (**8**) was cleavage inactive in visible light in the absence of any electronic band in the visible region. The results suggest the possible involvement of a metal-assisted photoexcitation process in the visible light-induced DNA-cleavage activity of the dpq complexes of Co(II) (**5**) and Cu(II) (**7**).

The DNA-cleavage activity of the dpq complexes was studied in the presence of several additives to determine the mechanistic pathway(s) involved in the photoinduced DNA-cleavage reactions (Figure S24 in the Supporting Information). In our earlier communication, we have shown that **7** cleaves DNA under aerobic conditions by a type-II pathway involving the formation of singlet oxygen ($^1O_2$) as the reactive species.[14] The present complexes are cleavage inactive in dark, indicating no apparent hydrolytic cleavage of DNA. Like the Cu(II) complex, the Co(II), Ni(II), and Zn(II) complexes did not show any photocleavage of DNA under argon atmosphere, indicating the necessity of molecular oxygen for the DNA-photocleavage reaction. Enhancement of the DNA cleavage in D_2O[48] and inhibition in the presence of sodium azide suggest the possible involvement of singlet oxygen as the reactive species. The complexes showed no inhibition in the DNA-cleavage activity in the presence of the hydroxyl radial scavengers like KI, DMSO, catalase, or superoxide radical scavenger SOD. The mechanistic data thus exclude the photoredox pathway forming any hydroxyl ($^{\bullet}OH$) and/or superoxide radical ($O_2^{\bullet-}$) in the photocleavage reaction (Figure S24 in the Supporting Information). The results are of significance as the binary dpq complexes of Co(II) and Cu(II) are known to photocleave DNA in visible light by a photoredox pathway in preference to the type-II pathway.[46,49] The groove selectivity of the complexes was determined from the control experiments using minor groove binder distamycin-A. Significant inhibition of the DNA-cleavage activity of the complexes has been observed in the

(45) Toshima, K.; Takano, R.; Ozawa, T.; Matsumura, S. *Chem. Commun.* **2002**, 212.

(46) Roy, M.; Pathak, B.; Patra, A. K.; Jemmis, E. D.; Nethaji, M.; Chakravarty, A. R. *Inorg. Chem.* **2007**, *46*, 11122.

(47) The photo-induced DNA-cleavage activity of $[M(dpq)_3]^{2+}$ [M = Fe(II), Co(II), Ni(II), Zn(II)] and $[Cu(dpq)_2(H_2O)]^{2+}$ shows that the Fe(II) and Ni(II) complexes are poor cleaver of DNA in visible light, whereas their Co(II) and Cu(II) analogues are efficient DNA cleavers via hydroxyl radical pathway (ref 46). Computational studies on these complexes reveal that a photo-redox DNA-cleavage pathway is more favorable for the Co(II) ($t_{2g}^5e_g^2$) and d^9-Cu(II) species in visible light. The same cleavage pathway is energetically unfavorable for the iron(II) ($t_{2g}^6e_g^0$) and Ni(II) ($t_{2g}^6e_g^2$) complexes. Because the present complexes cleave DNA via singlet oxygen mechanism in preference to the hydroxyl radical pathway, a detailed theoretical study is required to explain the poor cleavage activity of the Ni(II) complex, whereas the Co(II) analogue is active.

(48) (a) Khan, A. U. *J. Phys. Chem.* **1976**, *80*, 2219. (b) Merkel, P. B.; Kearns, D. R. *J. Am. Chem. Soc.* **1972**, *94*, 1029.

(49) Dhar, S.; Senapati, D.; Reddy, P. A. N.; Das, P. K.; Chakravarty, A. R. *Chem. Commun.* **2003**, 2452.

presence of distamycin-A-bound SC DNA, indicating the minor groove binding nature of the complexes (Figure S24 in the Supporting Information).

Conclusions

In summary, we present the hitherto unknown chemistry of 3d-metal scorpionates having dipyridoquinoxaline as a photoactive ligand showing DNA-cleavage activity in UV-A and visible light. Crystal structures of the complexes show a spatial arrangement of three phenyl groups of Tp^{Ph}, forming a bowl-shaped structure that effectively encloses the {M(B)} moiety. The steric encumbrance has a profound effect on the DNA binding, chemical nuclease, and photoinduced DNA-cleavage activity of the complexes. The steric encumbrance has led to reduced chemical nuclease but enhanced photoinduced DNA-cleavage activity of the Co(II) and Cu(II) complexes. The Co(II) and Cu(II) complexes of the dipyridoquinoxaline ligand show efficient visible light-induced DNA cleavage in a metal-assisted photoexcitation process in the presence of metal-centered visible band. The Ni(II) complex with its visible band having very low ε value and the Zn(II) complex in the absence of any visible band do not show any significant photoinduced DNA-cleavage activity in visible light. The photocleavage reactions of the Co(II) and Cu(II) complexes follow an oxidative type-II process involving the formation of singlet oxygen, whereas, in contrast, the binary dpq complexes of these metal ions are known to follow the photoredox pathway, generating reactive hydroxyl radicals.[46,49] The enhancement of cleavage activity on steric protection of the photosensitizer by the metal scorpionate moiety is of significance as it offers further scope of designing and tailoring new photosensitizers for potential phototherapeutic applications in PDT.

Acknowledgement. We thank the Department of Science and Technology, Government of India, for financial support (SR/S1/IC-10/2004) and the CCD diffractometer facility. We also thank the Council of Scientific and Industrial Research, New Delhi, for research fellowships to S.R. and A.K.P. We are grateful to the Alexander von Humboldt Foundation, Germany, for an electrochemical system and the Convener, Bioinformatics Center of our Institute, for database search.

Supporting Information Available: ESI-MS, unit cell packing diagrams for **4**−**6** and **8**, DNA-binding plots from absorption spectral titration, DNA melting plots, viscosity plots, emission binding plots, electronic spectra, gel electrophoresis diagrams (chemical nuclease activity, photoinduced DNA-cleavage activity at 365 nm, and in visible light), mechanistic details of the photocleavage reactions (S24), selected bond length and bond distances, full crystallographic data, atomic coordinates, full list of bond distances and angles, anisotropic thermal parameters, and hydrogen atom coordinates for **4**, **5**·Et_2O, **6**·$2H_2O$, and **8**·$2H_2O$ (CIF). This material is available free of charge via the Internet at http://pubs.acs.org.

IC702508R